

Color-Octet J/ψ Production in Υ Decay near the Kinematic Limit

Xiaohui Liu¹

¹*Department of Physics and Astronomy,
University of Pittsburgh, Pittsburgh, PA 15260*

(Dated: December 15, 2018)

Abstract

Recent experiments by the CLEO III detector at CESR indicate that the J/ψ spectrum produced in Υ decay is in conflict with Non-Relativistic QCD (NRQCD) calculations. The measured J/ψ momentum distribution is much softer than predicted by the color-octet mechanisms. The expected peak at the kinematic limit is not observed in the data. However it has recent been pointed out that NRQCD calculations break down near the kinematic endpoint due to large perturbative and non-perturbative corrections. In this paper we combine NRQCD with soft collinear effective theory to study the color-octet contribution to the $\Upsilon \rightarrow J/\psi + X$ decay in this region of phase space. We obtain a spectrum that is significantly softened when including the correct degrees of freedom in the endpoint region, giving better agreement with the data than previous predictions.

I. INTRODUCTION

Since the discovery of the J/ψ , heavy quarkonium decay and production have served as a laboratory for testing both perturbative and nonperturbative aspects of QCD dynamics. The large mass m_Q of the heavy quark inside the quarkonium set a high mass scale ($\sim 2m_Q$) at which the QCD approaches the asymptotically free regime and thus one could hope to calculate perturbatively. On the other hand, hadronization process happens at the much smaller mass scale of order $m_Q v^2$, where v is the typical velocity of the heavy quarks in the quarkonium. For quarkonium, $m_Q v^2$ is numerically of order Λ_{QCD} so the involved QCD process also contains nonperturbative effects.

During the past 15 years, the interactions of the non-relativistic heavy quarks inside the quarkonium have been understood to some extent using the framework of Non-Relativistic QCD (NRQCD) [1, 2]. NRQCD is an effective theory that reproduces the physics of full QCD by adding local interactions that systematically incorporate relativistic corrections through any given order in the heavy quark velocity v . This effective theory provides a generalized factorization theorem that includes nonperturbative corrections to the color-singlet model, including color-octet decay mechanisms. All infrared divergences can be factored into nonperturbative matrix elements, so that infrared safe calculations of inclusive decay rates are possible [3]. NRQCD solves some important phenomenological problems in quarkonium physics. For instance, it provides the most convincing explanation to the surplus J/ψ and ψ' production at the Tevatron [4], in which a gluon fragments into a color-octet $c\bar{c}$ pair in a pointlike color-octet S-wave state which evolves nonperturbatively into the charmonium states plus light hadrons. The NRQCD factorization formalism allows these fragmentation procedures to be factored into the product of short distance coefficients and long distance NRQCD matrix elements among which the leading one is $\langle \mathcal{O}_{\psi(\psi')}^8 [^3S_1] \rangle$ where $\mathcal{O}_{\psi(\psi')}^8$ are local 4-fermion operators in terms of the fields of NRQCD.

There are, however, some problems that remain to be solved. One challenging problem is with the polarization of J/ψ at the Tevatron. The same mechanism that produces the J/ψ described above predicts the J/ψ should become transversely polarized as the transverse momentum p_\perp becomes much larger than $2m_c$ [5]. Though the theoretical prediction is consistent with the experimental data at intermediate p_\perp , at the largest measured values of p_\perp the J/ψ is observed to be slightly longitudinally polarized and discrepancies at the 3σ level are seen in both prompt J/ψ and ψ' polarization measurements [6].

Recently, a new problem arose as a result of measurements of the spectrum of J/ψ produced in the $\Upsilon(1S)$ decay by the CLEO III detector at CESR [7]. NRQCD calculations have been made for the production of J/ψ through both color-singlet and color-octet configurations [8, 9]. Theoretical calculations predict that the color-singlet process $\Upsilon(1S) \rightarrow J/\psi c\bar{c}g + X$ features a soft momentum spectrum. Meanwhile, the theoretical estimates based on color-octet contribution indicates that the momentum spectrum peaks near the kinematic endpoint [9]. In contrast to the theoretical predictions, the experimentally measured momentum spectrum is significantly softer than predicted by the color-octet model and somewhat softer than the color-singlet case [7].

The NRQCD predictions break down in the endpoint region because the effective field theory does not contain the correct degrees of freedom to describe the physics. NRQCD contains soft quarks and gluons, but it does not contain quarks and gluons moving collinearly. The correct effective theory to use in situations where there is both soft and collinear physics is Soft-Collinear Effective Theory (SCET) [10–13]. A combination of SCET and NRQCD

has been successful in reproducing the shape of the measured J/ψ momentum spectrum in $e^+e^- \rightarrow J/\psi + X$ [14]. SCET has the power to describe the endpoint regime by including the light energetic degrees of freedom. In addition, renormalization group equations of SCET can be used to resum large perturbative logarithmic corrections. Nonperturbative matrix will occur naturally in deriving the factorization theorem using SCET.

In this paper, we use SCET to study the color-octet contribution to the $\Upsilon \rightarrow J/\psi + X$ decay near the endpoint. We derive the factorization theorem in SCET for this process. We find that the spectrum is significantly softened when including perturbative up to leading logarithms (LL) and nonperturbative corrections near the endpoint, giving better agreement with the data than the previous predictions.

II. FACTORIZATION AND MATCHING

In this section, we briefly derive the SCET factorization theorem for $\Upsilon \rightarrow J/\psi + X$ near the endpoint. A more detailed derivation will be presented in the Appendix. The derivation is similar to radiative Υ decay [16], which we refer to for details. However, for the process we discussed here, it involves the decay of a heavy quarkonium into another heavy quarkonium, thus we should combine SCET with two independent NRQCD's for these two onia systems. The factorization for a similar process $B \rightarrow J/\psi + X_s$ has been discussed in Ref. [15].

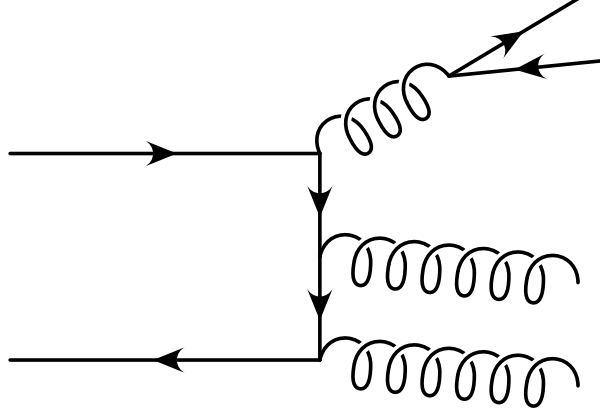
Near the endpoint regime, a new factorization formula is required since the NRQCD does not include all the relevant physical degrees of freedom and thus the factorization theorem breaks down. This can easily be seen when we analyze the kinematics at the endpoint. To do so, we work in the centre-of-mass (COM) frame, and introduce light cone coordinates. By introducing the parameter $x = (E_\psi + p_\psi)/M_\Upsilon$, we have

$$\begin{aligned} p_\Upsilon^\mu &= \frac{M_\Upsilon}{2} n^\mu + \frac{M_\Upsilon}{2} \bar{n}^\mu + k_\Upsilon^\mu, \\ p_\psi^\mu &= \frac{M_\psi^2}{2xM_\Upsilon} n^\mu + \frac{xM_\Upsilon}{2} \bar{n}^\mu + k_\psi^\mu, \\ p_X^\mu &= \frac{M_\Upsilon}{2} \left[\left(1 - \frac{r}{x}\right) n^\mu + (1-x)\bar{n}^\mu \right] + k_X^\mu. \end{aligned} \quad (1)$$

Here $n = (1, 0, 0, 1)$ and $\bar{n} = (1, 0, 0, -1)$, we have defined $r = m_c^2/m_b^2$, and we also assumed that $M_\psi = 2m_c$ and $M_\Upsilon = 2m_b$. k_Υ^μ and k_ψ^μ are the residual momentum of the $Q\bar{Q}$ pair inside the Υ and J/ψ respectively. Near the kinematic endpoint, the variable $x \rightarrow 1$ and thus the jet invariant mass approaches zero. In NRQCD, an expansion of k^μ/m_X is performed and hence the jet mode is integrated out, which is only valid when it has a large invariant mass, i.e., away from the endpoint. As $x \rightarrow 1$, the jet energy is large, but the invariant mass becomes small, with k^μ/m_X of order 1. Hence we must keep k^μ/m_X to all orders. As a result, the standard NRQCD factorization breaks down at the endpoint. SCET is the appropriate framework for properly including the collinear modes needed in the endpoint in order to make reasonable predictions.

To derive the factorization theorem in SCET, we start from the optical theorem in which the decay rate can be written as

$$2E_\psi \frac{d\Gamma}{d^3p_\psi} = \frac{1}{16\pi^3 M_\Upsilon} \sum_X \int d^4y e^{-iq \cdot y} \langle \Upsilon | \mathcal{O}^\dagger(y) | J/\psi + X \rangle \langle J/\psi + X | \mathcal{O}(0) | \Upsilon \rangle, \quad (2)$$



+ perms

FIG. 1: QCD production amplitude for $\Upsilon \rightarrow J/\psi + X$. The J/ψ is produced in a color-octet and becomes a color-singlet by emitting a soft gluon. There is another contribution to this process with only one gluon emitted, which is suppressed by an order of α_s .

where the summation includes integration over phase space of X . The SCET operator \mathcal{O} is

$$\mathcal{O} = \sum_i \sum_{\omega} e^{-i(M_{\Upsilon} v + \bar{P}_{\frac{\omega}{2}}) \cdot y} C_i(\mu, \omega) \mathcal{J}_i(\omega), \quad (3)$$

where the Wilson coefficient C_i is obtained by matching from QCD to SCET at some hard scale $\mu = \mu_H$ and the SCET current function $\mathcal{J}_i(\omega)$ is constrained by the gauge invariance. For instance, in our case, to leading order the non-vanishing SCET current will be of the form

$$\mathcal{J}(\omega) = \Gamma_{abc}^{\alpha\beta\mu\nu} [B_{\alpha, \omega_1}^{a\perp} B_{\beta, \omega_2}^{b\perp}] [\chi_b^\dagger (\Lambda_1 \cdot \sigma)_\nu \psi_b] [\chi_c^\dagger (\Lambda_2 \cdot \sigma)_\mu T^c \psi_c]. \quad (4)$$

Here $\Gamma_{abc}^{\alpha\beta\mu\nu}$ is a hard coefficient containing the color and spin structures which is obtained by matching onto the QCD Feynman diagrams shown in fig. 1. The matching gives

$$\Gamma_{abc}^{\alpha\beta\mu\nu} = \frac{2ig^4}{N_c} \frac{1}{1-r} \frac{M_\psi}{M_\Upsilon} \frac{1}{M_\psi^2} d_{abc} g_\perp^{\alpha\beta} (g_\perp^{\mu\nu} + \bar{n}^\mu n^\nu), \quad (5)$$

where we have chosen the coefficient so that the Wilson coefficient $C(\mu, \omega)$ is 1 at the hard scale μ_H . The Λ 's boost the J/ψ or Υ from the COM frame to a frame where those quarkonia have arbitrary four-momentum. ψ and χ are the heavy quark and antiquark fields which create or annihilate the constituent heavy (anti-)quarks inside the quarkonia. The collinear gauge invariant field strength is built out of the collinear gauge field $A_{n,q}^\mu$

$$B_\perp^\mu = \frac{-i}{g_s} W_n^\dagger (\mathcal{P}_\perp^\mu + g_s (A_{n,q}^\mu)_\perp) W_n, \quad (6)$$

where

$$W_n = \sum_{\text{perms}} \exp \left(-g_s \frac{1}{\mathcal{P}} \bar{n} \cdot A_{n,q} \right), \quad (7)$$

is the collinear Wilson line. The operator \mathcal{P} picks out the large momentum label [12].

We can decouple the usoft modes from the collinear degrees of freedom by making the field redefinition [13]

$$A_{n,q}^\mu \rightarrow Y A_{n,q}^\mu Y^\dagger, \quad (8)$$

where Y is the usoft Wilson line made out of the usoft gauge fields. In such a way, we can separate the collinear physics from the usoft and obtain the factorization theorem in SCET. Meanwhile using similar arguments presented in Ref. [15] allows us to factorize the matrix element into the convolution of the shape functions for Υ in color-singlet configuration and J/ψ in color-octet one. Following this procedure, the decay rates can be written as a convolution of soft shape functions and the jet function with an overall hard coefficient. By introducing $z = E_\psi/m_b$, we get the decay rate of the form

$$\frac{d\Gamma}{dz} = \Gamma_0 P[z, r] \sum_{\omega} |C(\omega, \mu)|^2 \int dk^+ \int dl^+ J_\omega(k^+) S_\psi(l^+) S_\Upsilon(M_\Upsilon(1-x) - k^+ - l^+), \quad (9)$$

where $P[z, r] = 8\pi\sqrt{z^2 - 4r}/(1-r)$ is a kinematic factor and

$$\Gamma_0 = \frac{\pi\alpha_s^4}{18} \frac{N_c^2 - 4}{N_c^3} \frac{2+r}{1-r} \frac{1}{m_b^2 m_c^3} \langle \Upsilon | \mathcal{O}_\Upsilon^1[{}^3S_1] | \Upsilon \rangle \langle \mathcal{O}_\psi^8[{}^3S_1] \rangle. \quad (10)$$

We have used spin symmetry [17]

$$\Lambda_i^\delta \Lambda_j^{\delta'} \langle \dots \sigma^i \dots \sigma^j \dots \rangle = \frac{1}{3} \delta^{ij} \Lambda_i^\delta \Lambda_j^{\delta'} \langle \dots \sigma^k \dots \sigma^k \dots \rangle, \quad (11)$$

to simplify the matrix elements, and applied the identity $\delta^{ij} \Lambda_i^\delta \Lambda_j^{\delta'} = (v^\delta v^{\delta'} - g^{\delta\delta'})$, where v^δ is the four-velocity of the Υ or J/ψ .

The shape function for J/ψ is defined as

$$S_\psi(l^+) = \int \frac{dy^-}{4\pi} e^{-\frac{i}{2}l^+y^-} \frac{\langle 0 | \left[\chi_{\bar{c}}^\dagger \sigma_i Y \tilde{Y} T^k \tilde{Y}^\dagger Y^\dagger \psi_c(y^-) a_\psi^\dagger a_\psi \psi_c^\dagger \sigma_i Y \tilde{Y} T^k \tilde{Y}^\dagger Y^\dagger \chi_{\bar{c}} \right] | 0 \rangle}{4m_c \langle \mathcal{O}_\psi^8[{}^3S_1] \rangle}, \quad (12)$$

where we have made the field redefinition in Eq. (8) for the two collinear gluons in the final state by introducing two different usoft Wilson lines Y and \tilde{Y} . For Υ we have the shape function

$$S_\Upsilon(l^+) = \int \frac{dy^-}{4\pi} e^{-\frac{i}{2}l^+y^-} \frac{\langle \Upsilon | \chi_b^\dagger \sigma_i \psi_b(y^-) \psi_b^\dagger \sigma_i \chi_{\bar{b}} | \Upsilon \rangle}{4m_b \langle \Upsilon | \mathcal{O}_\Upsilon^1[{}^3S_1] | \Upsilon \rangle} \quad (13)$$

respectively. Both shape functions are normalized so that $\int dl^+ S_{\psi, \Upsilon}(l^+) = 1$.

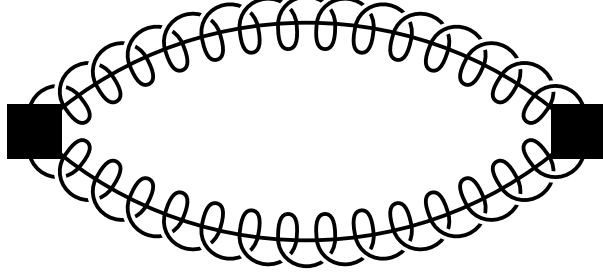


FIG. 2: Feynman diagram for the leading-order jet function. The spring with a line through it represents a collinear gluon.

The jet function is given by

$$\begin{aligned} & \langle 0 | \left[B_{\alpha}^{a\perp} B_{\beta}^{b\perp}(y) B_{\alpha'}^{a'\perp} B_{\beta'}^{b'\perp}(0) \right] | 0 \rangle \\ &= \frac{i}{2} (g_{\alpha\alpha'} g_{\beta\beta'} \delta^{aa'} \delta^{bb'} + g_{\alpha\beta'} g_{\beta\alpha'} \delta^{ab'} \delta^{ba'}) \delta_{\omega\omega'} \int \frac{dk^+}{2\pi} \delta^{(2)}(y^{\perp}) \delta(y^+) e^{-\frac{i}{2}k^+y^-} J_{\omega}(k^+). \end{aligned} \quad (14)$$

To the leading order, the jet function can be calculated by evaluating the diagram shown in Fig. 2, which gives

$$J_{\omega}(k^+) = \frac{1}{8\pi} \Theta(k^+) \int_0^1 d\xi \delta_{\xi, (\bar{n}Q+\omega)/(2\bar{n}Q)}, \quad (15)$$

where Q is the total four momentum carried by the jets.

The J/ψ shape function can formally be written as

$$S_{\psi}(l^+) = \frac{\langle 0 | \left[\chi_{\bar{c}}^{\dagger} \sigma_i Y \tilde{Y} T^k \tilde{Y}^{\dagger} Y^{\dagger} \psi_c \delta(in \cdot \partial - l^+) a_{\psi}^{\dagger} a_{\psi} \psi_c^{\dagger} \sigma_i Y \tilde{Y} T^k \tilde{Y}^{\dagger} Y^{\dagger} \chi_{\bar{c}} \right] | 0 \rangle}{4m_c \langle \mathcal{O}_{\psi}^8[{}^3S_1] \rangle}, \quad (16)$$

and to lowest order in v^2 , $S_{\Upsilon}(l^+) \rightarrow \delta(l^+)$. By integrating over k^+ and l^+ in Eq. (9), we find the tree level decay rates become

$$\frac{d\Gamma}{dz} = \Gamma_0 \tilde{P}[z, r] \Theta(1-x), \quad (17)$$

with $\tilde{P}[z, r] = P[z, r]/8\pi$. This can easily be seen to reproduce the tree level calculation of NRQCD [9].

III. RUNNING

Effective field theories provide a powerful tool to sum logarithms by using the renormalization group equations (RGEs). Logarithms of the ratio of different scales arise naturally in perturbation theory, which can cause a breakdown of the perturbative expansion when those scales are well separated. By matching onto an effective theory, the large scale is removed to be replaced by a running scale μ and the effective operators are run from a high scale to

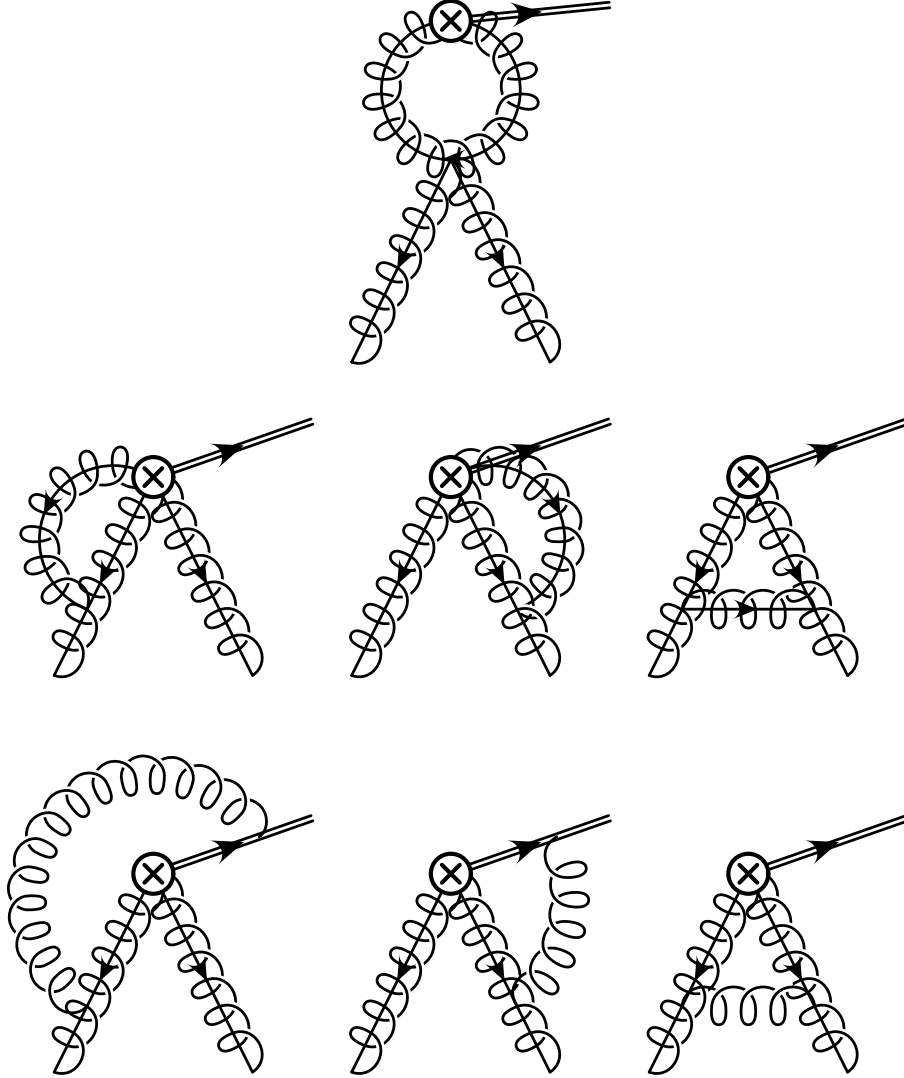


FIG. 3: One-loop order diagrams needed to calculate the counterterm to the color-octet operator. The double line presents the J/ψ fields in color-octet configuration while the spring lines are the soft gluons.

the low scale using the RGEs, which sum all large logarithms of the ratio of scales into an overall factor.

In our case, there are logarithms of the form $\log(1-x)$ that will appear in the perturbation series. Near the endpoint, $x \rightarrow 1$, these become large, and must be resummed. In this section, we will apply the RGEs of SCET to sum these large logarithms.

In the previous section, we have matched QCD onto the SCET operator by integrating out the hard scale μ_H , replacing it with a running scale μ . We now run the operator from this hard scale to the collinear scale. To do so, we calculate the counterterm for the operator to determine the anomalous dimension, and then use this in the RGEs.

The one-loop corrections to the SCET operator in Eq. (4) is given by the graphs in Fig. 3.

Evaluating these diagrams gives the divergent term

$$\begin{aligned} \mathcal{A}_{1\text{-loop}} = \sum_{\omega} \frac{\alpha_s C_A}{4\pi} \left\{ \left[\frac{1}{\epsilon^2} + \frac{1}{\epsilon} \left(2 + \log \frac{\mu^2}{\bar{n} \cdot Q^2 / r} \right) \right] \right. \\ \left. + \frac{1}{\epsilon} \left[\frac{\omega(\bar{n} \cdot Q + \omega)}{\bar{n} \cdot Q(\bar{n} \cdot Q - \omega)} \log \frac{\bar{n} \cdot Q + \omega}{2\bar{n} \cdot Q} - \frac{\omega(\bar{n} \cdot Q - \omega)}{\bar{n} \cdot Q(\bar{n} \cdot Q + \omega)} \log \frac{\bar{n} \cdot Q - \omega}{2\bar{n} \cdot Q} \right] \right\} \times \mathcal{A}_0. \end{aligned} \quad (18)$$

The calculation lets us estimate the hard scale be $\mu_H = \bar{n} \cdot Q / \sqrt{r}$ which will minimize the logarithm. The divergent piece must be canceled by $Z_8 Z_3 / Z_O - 1$, where Z_O is the counterterm for the operator in SCET, Z_3 is the gluon wave function counterterm

$$Z_3 = 1 + \frac{\alpha_s}{4\pi} \frac{1}{\epsilon} \left(\frac{5}{3} C_A - \frac{4n_F}{3} T_F \right), \quad (19)$$

and Z_8 is the counterterm of color-octet J/ψ operator

$$Z_8 = 1 + \frac{\alpha_s C_A}{4\pi\epsilon}. \quad (20)$$

This leads to

$$\begin{aligned} Z_O - 1 = \sum_{\omega} \frac{\alpha_s C_A}{4\pi} \left\{ \left[\frac{1}{\epsilon^2} + \frac{1}{\epsilon} \left(\log \frac{\mu^2}{\bar{n} \cdot Q^2 / r} \right) + \frac{1}{\epsilon} \left(\frac{14}{3} - \frac{4n_F}{3} \frac{T_F}{C_A} \right) \right] \right. \\ \left. + \frac{1}{\epsilon} \left(+ \frac{\omega(\bar{n} \cdot Q + \omega)}{\bar{n} \cdot Q(\bar{n} \cdot Q - \omega)} \log \frac{\bar{n} \cdot Q + \omega}{2\bar{n} \cdot Q} - \frac{\omega(\bar{n} \cdot Q - \omega)}{\bar{n} \cdot Q(\bar{n} \cdot Q + \omega)} \log \frac{\bar{n} \cdot Q - \omega}{2\bar{n} \cdot Q} \right) \right\}. \end{aligned} \quad (21)$$

From Eq. (21), we can extract the anomalous dimension of the operator through the standard method. Using the anomalous dimension in the RGE for the color-octet Wilson coefficient and running from the hard scale down to the collinear scale gives

$$|C(\xi, \mu_c)|^2 = \left[\frac{\mu_c^2}{\bar{n} \cdot Q^2 / r} \right]^{-\frac{2C_A}{b_0}} \left[\frac{\alpha_s(\mu_c^2)}{\alpha_s(\bar{n} \cdot Q^2 / r)} \right]^{-\frac{8\pi C_A}{\alpha_s(\bar{n} \cdot Q^2 / r) b_0^2}} \left[\frac{\alpha_s(\mu_c^2)}{\alpha_s(\bar{n} \cdot Q^2 / r)} \right]^{4\eta[\xi]}, \quad (22)$$

where

$$\eta[\xi] = \frac{C_A}{2b_0} \left[\left(\frac{14}{3} - \frac{4n_F}{3} \frac{T_F}{C_A} \right) - (2\xi - 1) \left(\frac{1-\xi}{\xi} \log(1-\xi) - \frac{\xi}{1-\xi} \log \xi \right) \right], \quad (23)$$

with $\xi = (\bar{n} \cdot Q + \omega) / (2\bar{n} \cdot Q)$, $b_0 = 11C_A/3 - 2n_F/3$, and the collinear scale $\mu_c^2 \approx m_X^2$.

At the collinear scale, the jet mode can be regarded as large and can be integrated out. The decay rate can be further run down to the soft scale μ_s . To do this, we first note that the decay rate can be modified to

$$\frac{d\Gamma}{dz} = \Gamma_0 \tilde{P}[z, r] \int_0^1 d\xi |C(\xi, \mu_c)|^2 \int dl^+ dl'^+ \Theta(M_T(1-x) - l^+) \mathcal{U}_s(l^+ - l'^+, \mu_c, \mu_s) S_\psi(l'^+, \mu_s), \quad (24)$$

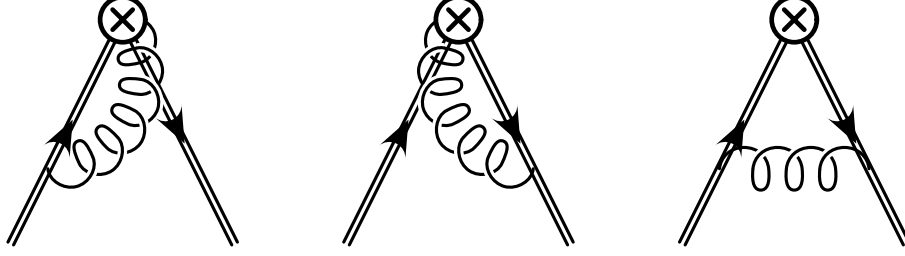


FIG. 4: One loop corrections to the J/ψ soft shape function defined in Eq. (12).

since in Ref. [18], it was shown that

$$\langle \Upsilon | \chi_b^\dagger \sigma_i \psi_b \Theta(in \cdot \partial + M_\Upsilon(1-x) - l^+) \psi_b^\dagger \sigma_i \chi_{\bar{b}} | \Upsilon \rangle = \Theta(M_\Upsilon(1-x) - l^+) \langle \Upsilon | \chi_b^\dagger \sigma_i \psi_b \psi_b^\dagger \sigma_i \chi_{\bar{b}} | \Upsilon \rangle. \quad (25)$$

And here we introduced an evolution kernel \mathcal{U}_s as in Ref. [19]. The soft shape function has evolution through \mathcal{U}_s which will sum the large logarithms between μ_s and μ_c .

The evolution kernel can be calculated explicitly [19], once we figure out the anomalous dimension for the soft shape function. To one-loop order, calculating the diagrams in fig. 4, we get

$$Z_{S_\psi} - 1 = \frac{\alpha_s}{2\pi} C_A \left[\left(-\frac{1}{\epsilon^2} - \frac{1}{\epsilon} \log \frac{\mu^2}{r M_\Upsilon^2} + \frac{1}{\epsilon} \right) \delta(k^+) + \frac{2}{\epsilon} \frac{1}{M_\Upsilon} \left(\frac{M_\Upsilon \Theta(k^+)}{k^+} \right)_+ \right]. \quad (26)$$

Therefore we \mathcal{U}_s is

$$\mathcal{U}_s(l^+ - l'^+) = \frac{e^{\tilde{K}} (e^{\gamma_E})^{\tilde{\omega}}}{\mu_s \Gamma(-\tilde{\omega})} \left[\frac{\mu_s^{1+\tilde{\omega}} \Theta(l^+ - l'^+)}{(l^+ - l'^+)^{1+\tilde{\omega}}} \right]_+, \quad (27)$$

with $\tilde{\omega}$ is defined as

$$\tilde{\omega} = -\frac{2C_A}{\pi} \int_{\alpha_s(\mu_s)}^{\alpha_s(\mu_c)} \frac{\alpha d\alpha}{\beta[\alpha]} = \frac{4C_A}{b_0} \log \frac{\alpha_s(\mu_c)}{\alpha_s(\mu_s)}, \quad (28)$$

where $\beta[\alpha_s] = -(11C_A/3 - 2n_F/3)\alpha_s^2/(2\pi)$. Note that $\tilde{\omega} < 0$. We defined a function \tilde{K}_γ

$$\tilde{K}_\gamma = \frac{C_A}{\pi} \int_{\alpha_s(\mu_s)}^{\alpha_s(\mu_c)} \frac{\alpha d\alpha}{\beta[\alpha]} (1 + \log r) = -\frac{2C_A}{b_0} (1 + \log r) \log \frac{\alpha_s(\mu_c)}{\alpha_s(\mu_s)}, \quad (29)$$

which is related to \tilde{K} in Eq. (27) by

$$\begin{aligned} \tilde{K} &= \tilde{K}_\gamma - \frac{2C_A}{\pi} \int_{\alpha_s(\mu_s)}^{\alpha_s(\mu_c)} \frac{\alpha d\alpha}{\beta[\alpha]} \int_{\alpha_s(\mu_s)}^{\alpha} \frac{d\alpha'}{\beta[\alpha']} \\ &= \tilde{K}_\gamma + \frac{8\pi C_A}{b_0^2 \alpha_s(\mu_c)} \left(\frac{\alpha_s(\mu_c)}{\alpha_s(\mu_s)} - 1 - \frac{\alpha_s(\mu_c)}{\alpha_s(\mu_s)} \log \frac{\alpha_s(\mu_c)}{\alpha_s(\mu_s)} \right). \end{aligned} \quad (30)$$

The soft scale is $\mu_s^2 \sim r M_\Upsilon^2 (1-x)^2$.

Gathering all the pieces we have, we find the resummed decay rate

$$\begin{aligned} \frac{d\Gamma}{dz} = & \Gamma_0 \tilde{P}[z, r] \left[\frac{\mu_c^2}{\bar{n} \cdot Q^2 / r} \right]^{-\frac{2C_A}{b_0}} \left[\frac{\alpha_s(\mu_c^2)}{\alpha_s(\bar{n} \cdot Q^2 / r)} \right]^{-\frac{8\pi C_A}{\alpha_s(\bar{n} \cdot Q^2 / r) b_0^2}} \int_0^1 d\xi \left[\frac{\alpha_s(\mu_c^2)}{\alpha_s(\bar{n} \cdot Q^2 / r)} \right]^{4\eta[\xi]} \\ & \times \frac{e^{\tilde{K}}(e^{\gamma_E})^{\tilde{\omega}}}{\mu_s \Gamma(-\tilde{\omega})} \int dl^+ dl'^+ \Theta(M_\Upsilon(1-x) - l^+) \left[\frac{\mu_s^{1+\tilde{\omega}} \Theta(l^+ - l'^+)}{(l^+ - l'^+)^{1+\tilde{\omega}}} \right]_+ S_\psi(l'^+, \mu_s). \end{aligned} \quad (31)$$

IV. PHENOMENOLOGY

The decay rate from the previous section, Eq. (31), summed up the leading logarithmic corrections which are important near the kinematic endpoint. Away from that region, the logarithms that we have summed are not important and contributions that we neglected in the endpoint become important. We therefore would like to interpolate between the leading order color-octet contribution in NRQCD away from the endpoint and the resummed result near the endpoint. We thus define the interpolated differential rate as

$$\frac{d\Gamma}{dy} = (1-y) \left(\frac{d\Gamma}{dy} \right)_{\text{NRQCD}} + y \left(\frac{d\Gamma}{dy} \right)_{\text{SCET}}. \quad (32)$$

Here, in order to compare with the data, we have used the scaled momentum defined as $y = p_\psi / p_\psi^{\text{max}}$. We see that as $y \rightarrow 1$ the first term vanishes, leaving only the SCET contribution in the endpoint region.

To proceed, we need the soft shape function of J/ψ that appears in Eq. (31). We will apply a modified version of a model used in the decay of B mesons [20],

$$f(\hat{l}^+) = \frac{1}{\Lambda} \frac{a^{ab}}{\Gamma(ab)} (\eta - 1)^{ab-1} e^{-a(\eta-1)} \Theta(\eta - 1), \quad (33)$$

with $\eta = \hat{l}^+ / \Lambda$. Here $\Lambda = M_\psi - M$ is of order Λ_{QCD} , and a and b are adjustable parameters of order 1. In our case, we choose $a = 1$ and $b = 2$. Λ was determined so that the first and the second moments of the shape function

$$\begin{aligned} m_1 &= \int_\Lambda^\infty d\hat{l}^+ f(\hat{l}^+) = \Lambda(b+1), \\ m_2 &= \int_\Lambda^\infty d\hat{l}^+ (\hat{l}^+)^2 f(\hat{l}^+) = \Lambda^2 \left(\frac{b}{a} + (b+1)^2 \right), \end{aligned} \quad (34)$$

take the value 890 MeV and (985 MeV)² respectively.

We show the results of resumming in fig. 5. The short dashed line is the NRQCD decay rate only and the dotted line is the NRQCD decay rate convoluted with the shape function. The thin line includes only the perturbative resummed interpolated decay rates without convoluted with the soft shape function. The solid thick line presenting our final result is the interpolated decay rate convoluted with the shape function in Eq. (33). As can be seen, the shape function and the perturbative resummation both result in a softer spectrum. The combination of the two is softer still.

In fig. 6, we compare our results with the experimental data from CLEO [7]. We use the values $m_c = 1.5$ GeV, $m_b = 4.9$ GeV, and $\Lambda_{\text{QCD}} = 0.2$ GeV so that $\alpha_s(2m_b) = 0.1793$.

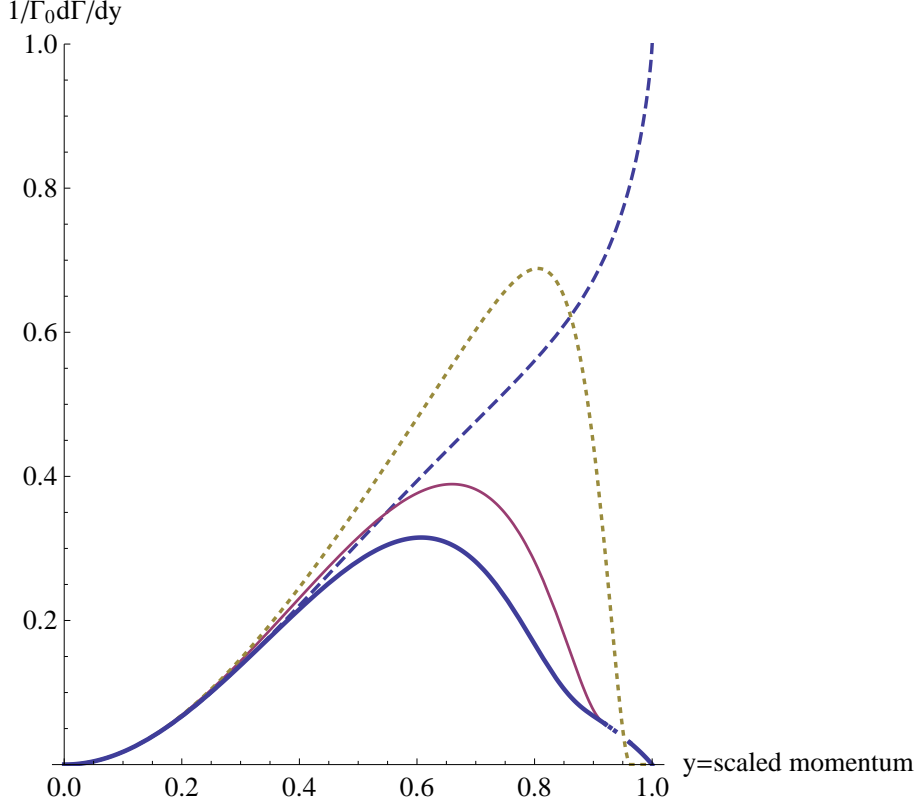


FIG. 5: Comparison between the NRQCD results and SCET predictions normalized to the NRQCD decay rate at the end-point. Here $y = p_\psi/p_\psi^{max}$ is the scaled momentum. The short dashed line is the NRQCD decay rate only and the dotted line is the NRQCD decay rate convoluted with the shape function. The solid thin line includes only the perturbative resummed interpolated decay rates without convoluted with the soft shape function. The solid thick line presents the interpolated decay rates convoluted with the shape function.

The solid line represents the color-octet interpolated decay rate convoluted with the shape function. The NRQCD matrix element was chosen to be $\langle \Upsilon | \mathcal{O}_\Upsilon^1[{}^1S_0] | \Upsilon \rangle = 2.3 \text{ GeV}^3$. For comparison, we have used in the plot the same value for the overall strong coupling evaluated at the scale $2m_c$ as in Ref. [9]. The shaded band is obtained by varying the NRQCD color-octet matrix element from 0.003 GeV^3 to 0.014 GeV^3 . Since the numerical value of the matrix element $\langle \mathcal{O}_\psi^8[{}^3S_1] \rangle$ is fixed by experimental data, it has large uncertainties coming both from experiments and theoretical higher order corrections. For comparison, we also show the color-singlet contribution as the dashed line [7, 8]. The complete spectrum involves a combination of the color-octet contribution we calculated here, and the color-singlet component [7, 8] shown in the figure.

The differential rate predicted by the color-octet model is peaked near the end-point region. When convoluted with the shape function, the momentum distribution is shifted to the left but still close to the kinematic limit. Once we resum the large leading logarithms under the framework of SCET, interpolate the result with the NRQCD prediction and then convolute with the soft shape function, we find that spectrum is significantly softened near the endpoint and the peak is pushed further to the left, in better agreement with the data.

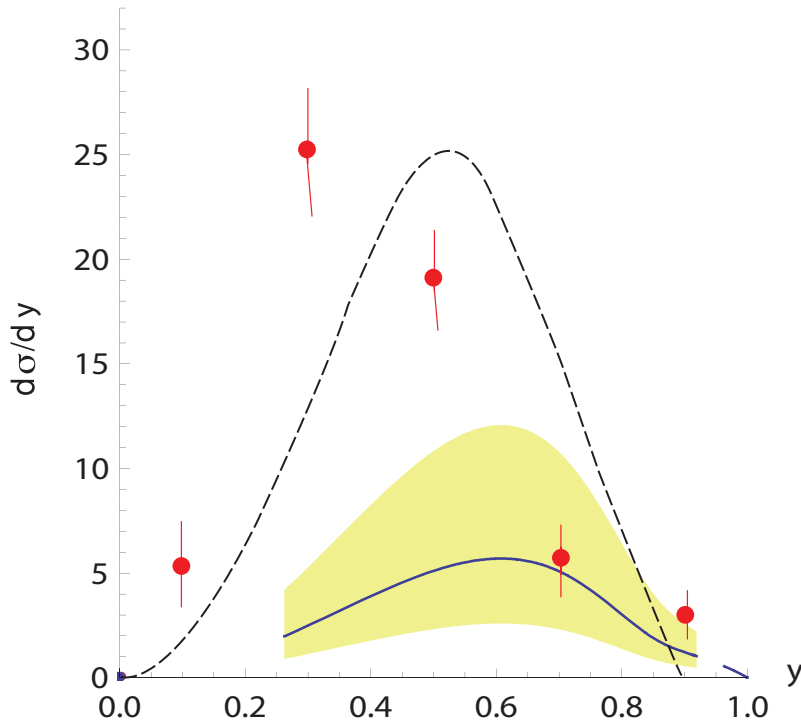


FIG. 6: Comparison of the color-octet contribution to the differential rate to the data from CLEO [7]. The solid thick line presents the interpolated decay rates convoluted with the shape function with a choice of $\langle \mathcal{O}_\psi^8[{}^3S_1] \rangle = 6.6 \times 10^{-3} \text{GeV}^3$ [21]. The shaded band is obtained by varying $\langle \mathcal{O}_\psi^8[{}^3S_1] \rangle$ from 0.003GeV^3 to 0.014GeV^3 [22]. Here, we also show the color-singlet contribution in long dashed line [7, 8]. The complete spectrum will involve a combination of both the color-octet and color-singlet contributions.

We note here that if we use a high scale for the overall coupling constant, the color-octet contribution will be much smaller. In order to make a consistent comparison of theory to data, one needs to treat the endpoint of the color-singlet contribution in SCET and NRQCD, which we have not done here and will leave for future work. In the perturbative expansion, the color-singlet process is suppressed relative to the color-octet one by a factor of α_s . However, there is a large enhancement due to kinematic factors in the diagram, which can be as large as 360 that provides a huge enhancement to compensate the perturbative suppression [8].

V. CONCLUSION

In this paper we studied the color-octet contribution to $\Upsilon \rightarrow J/\psi + X$ near the kinematic endpoint. In this regime, the usual NRQCD factorization formalism breaks down due to large perturbative and nonperturbative corrections. We combined the usual NRQCD effective theory with SCET, which contains the correct physical degrees of freedom, to derive a factorization theorem for the differential decay rate, $d\Gamma/dy$, valid in the endpoint region.

This also allows us to resum large logarithms which appear in the endpoint by running the rate from the hard scale to the collinear scale and then to the soft scale using the RGE of the effective theory. At the soft scale, we are left with NRQCD shape functions. Using models for the color-octet shape function, and interpolating away from the endpoint to the leading order NRQCD prediction, we are able to make predictions about the color-octet contribution to the decay rate over the entire kinematic region.

Though a quantitative comparison to data can be made only when including both the color-singlet and color-octet terms, some qualitative conclusions can still be drawn here. We note that once we sum the large leading logarithms using the framework of SCET and convolute with the soft shape function, the spectrum is significantly softened near the endpoint and the peak is broadened and shifted to the left. This effect greatly improves the agreement between the data constraints and the theoretical predictions.

We note here that the hard scale we have chosen in our final results is $2m_c$ the same as in [9]. This scale is much smaller than what we expected from our one loop order corrections. If we used the hard scale μ_H decided by our calculations, the color-octet contribution will be further suppressed. As a result, we expected that the dominant contribution for this process will be from color-singlet rate. Once including higher order effects as well as the feed-down of $\psi(2S)$ and χ_{cJ} to J/ψ [7], the color-singlet decay rate should also be softened. We expected that combining color-singlet and octet contributions will give a good fit to the data.

VI. ACKNOWLEDGEMENTS

I am grateful to Professor A. K. Leibovich for guidances and carefully reading the manuscript and checking all the calculations. XL was supported in part by the National Science Foundation under Grant No. PHY-0546143.

Appendix A: Deriving The Factorization Theorem for the Endpoint

In this Appendix we show the factorization theorem for $\Upsilon \rightarrow J/\psi + X$ near the endpoint. We begin with the differential decay rate

$$2E_\psi \frac{d\Gamma}{d^3p_\psi} = \frac{1}{16\pi^3 M_\Upsilon} \sum_X \int d^4y e^{-iq \cdot y} \langle \Upsilon | \mathcal{O}^\dagger(y) | J/\psi + X \rangle \langle J/\psi + X | \mathcal{O}(0) | \Upsilon \rangle, \quad (\text{A1})$$

where X includes both the usoft X_u sector and the collinear X_c sector. The operator \mathcal{O} is the SCET operator defined in Section II of the form

$$\mathcal{O} = e^{-i(M_\Upsilon v + \bar{P} \frac{n}{2}) \cdot y} \Gamma_{abc}^{\alpha\beta\mu\nu} \mathcal{J}_{\alpha\beta}^{ab} \mathcal{O}_\nu^\Upsilon[\mathbf{1}^3 S_1] \mathcal{O}_\mu^{c\psi}[\mathbf{8}^3 S_1], \quad (\text{A2})$$

where

$$\mathcal{J}_{\alpha\beta}^{ab} = B_{\alpha,\omega_1}^{a\perp} B_{\beta,\omega_2}^{b\perp}, \quad (\text{A3})$$

$$\mathcal{O}_\nu^\Upsilon[\mathbf{1}^3 S_1] = \psi_b^\dagger (\Lambda_1 \cdot \sigma)_\nu \chi_{\bar{b}}, \quad (\text{A4})$$

$$\mathcal{O}_\mu^{c\psi}[\mathbf{8}^3 S_1] = \psi_c^\dagger (\Lambda_2 \cdot \sigma)_\mu T^c \chi_{\bar{c}}. \quad (\text{A5})$$

Inserting the operator into Eq. (A1), the $\mathcal{O}^\dagger(y)$ picks up an additional phase and the differential rate becomes

$$\begin{aligned}
2E_\psi \frac{d\Gamma}{d^3p_\psi} &= \frac{1}{16\pi^3 M_\Upsilon} \sum_X \int d^4y e^{-iM_\Upsilon/2(1-x)\cdot\bar{n}\cdot y} \Gamma_{abc}^{\alpha\beta\mu\nu\dagger} \Gamma_{a'b'c'}^{\alpha'\beta'\mu'\nu'} \\
&\times \langle \Upsilon | \mathcal{J}_{\alpha\beta}^{ab\dagger} \mathcal{O}_\nu^{\Upsilon\dagger}[\mathbf{1}^3 S_1] \mathcal{O}_\mu^{c\psi\dagger}[\mathbf{8}^3 S_1](y) | J/\psi + X \rangle \\
&\langle J/\psi + X | \mathcal{J}_{\alpha'\beta'}^{a'b'\dagger} \mathcal{O}_{\nu'}^{\Upsilon}[\mathbf{1}^3 S_1] \mathcal{O}_{\mu'}^{c'\psi}[\mathbf{8}^3 S_1](0) | \Upsilon \rangle \\
&\equiv \Gamma_{abc}^{\alpha\beta\mu\nu\dagger} \Gamma_{a'b'c'}^{\alpha'\beta'\mu'\nu'} \mathcal{A}_{\alpha\beta\mu\nu,\alpha'\beta'\mu'\nu'}^{abc,a'b'c'} .
\end{aligned} \tag{A6}$$

In the exponent of Eq. (A6), we have used $q^\mu - M_\Upsilon v^\mu + \bar{\mathcal{P}}n^\mu/2 \approx M_\Upsilon/2(1-x)\bar{n}^\mu$. As mentioned in Section II, we can decouple the usoft modes from the collinear degrees of freedom using the field redefinition [13]

$$A_{n,q}^\mu \rightarrow Y A_{n,q}^\mu Y^\dagger, \tag{A7}$$

which modifies $\mathcal{O}_\mu^{c\psi}[\mathbf{8}^3 S_1]$ to

$$\mathcal{O}_\mu^{c\psi} \rightarrow Y \tilde{Y} \mathcal{O}_\mu^{c\psi} \tilde{Y}^\dagger Y^\dagger \equiv \tilde{\mathcal{O}}_\mu^{c\psi}. \tag{A8}$$

Using this field redefinition, we can write

$$\begin{aligned}
\mathcal{A}_{\alpha\beta\mu\nu,\alpha'\beta'\mu'\nu'}^{abc,a'b'c'} &= \frac{1}{16\pi^3 M_\Upsilon} \int d^4y e^{-iM_\Upsilon/2(1-x)\bar{n}\cdot y} \\
&\times \langle \Upsilon | \mathcal{O}_\nu^{\Upsilon\dagger}[\mathbf{1}^3 S_1] \tilde{\mathcal{O}}_\mu^{c\psi\dagger}[\mathbf{8}^3 S_1](y) a_\psi^\dagger a_\psi \mathcal{O}_{\nu'}^{\Upsilon}[\mathbf{1}^3 S_1] \tilde{\mathcal{O}}_{\mu'}^{c'\psi}[\mathbf{8}^3 S_1](0) | \Upsilon \rangle \\
&\times \langle 0 | \mathcal{J}_{\alpha\beta}^{ab\dagger}(y) \mathcal{J}_{\alpha'\beta'}^{a'b'\dagger}(0) | 0 \rangle,
\end{aligned} \tag{A9}$$

where we have introduced an interpolating field, a_ψ , for the J/ψ and used the completeness of states in the usoft and collinear sectors

$$\sum_{X_u} |J/\psi + X_u\rangle \langle J/\psi + X_u| = a_\psi^\dagger \sum_{X_u} |X_u\rangle \langle X_u| a_\psi = a_\psi^\dagger a_\psi, \tag{A10}$$

$$\sum_{X_c} |X_c\rangle \langle X_c| = 1. \tag{A11}$$

The the usoft Wilson lines only come with the color-octet J/ψ operator, $\mathcal{O}_\mu^{c\psi}[\mathbf{8}^3 S_1]$. The Υ is a very compact bound state, due to the large b -quark mass. In a multipole expansion, long wavelength gluons interacts with the Υ color charge distribution through its color dipole moment since the state itself is color neutral. In the theoretical limit of very heavy bottom quark, this coupling to the dipole vanishes [15]. The order of the corrections can be estimated by means of the ‘‘vacuum-saturation approximation’’ [1]. A complete set of light-hadronic states $\sum_X |X\rangle \langle X|$ can be inserted between the Υ operator and the J/ψ operator. Notice that the Υ operator is in color-singlet configuration. therefore the sum over states is saturated by the QCD vacuum $|0\rangle$ with corrections of order v^4 [1].

Thus we are able to write

$$\begin{aligned}
\mathcal{A}_{\alpha\beta\mu\nu,\alpha'\beta'\mu'\nu'}^{abc,a'b'c'} &\approx \frac{1}{16\pi^3 M_\Upsilon} \int d^4y e^{-iM_\Upsilon/2(1-x)\bar{n}\cdot y} \\
&\times \langle \Upsilon | \mathcal{O}_\nu^{\Upsilon\dagger}[\mathbf{1}^3 S_1](y) \mathcal{O}_{\nu'}^{\Upsilon}[\mathbf{1}^3 S_1](0) | \Upsilon \rangle \\
&\times \langle 0 | \tilde{\mathcal{O}}_\mu^{c\psi\dagger}[\mathbf{8}^3 S_1](y) a_\psi^\dagger a_\psi \tilde{\mathcal{O}}_{\mu'}^{c'\psi}[\mathbf{8}^3 S_1](0) | 0 \rangle \\
&\times \langle 0 | \mathcal{J}_{\alpha\beta}^{ab\dagger}(y) \mathcal{J}_{\alpha'\beta'}^{a'b'\dagger}(0) | 0 \rangle.
\end{aligned} \tag{A12}$$

Now we substitute the expressions for the Υ and J/ψ shape functions as well as the jet function from Section II into Eq. (A12), and use $p_\psi^2 dp_\psi / (2E_\psi) = m_b^2 \sqrt{z - 4r} dz / 2$. The result for differential decay rate becomes

$$\frac{d\Gamma}{dz} = \Gamma_0 P[z, r] \sum_{\omega} |C(\omega, \mu)|^2 \int dk^+ \int dl^+ J_{\omega}(k^+) S_{\psi}(l^+) S_{\Upsilon}(M_{\Upsilon}(1-x) - k^+ - l^+) \quad (\text{A13})$$

Thus we obtain the desired factorization theorem in the endpoint region.

-
- [1] G. T. Bodwin, E. Braaten and G. P. Lepage, Phys. Rev. D **51** 1125 (1995).
 - [2] M. E. Luke, A. V. Manohar and I. Z. Rothstein, Phys. Rev. D **61** 074025 (2000).
 - [3] G. T. Bodwin, E. Braaten and G. P. Lepage, Phys. Rev. D **46** 1914 (1992).
 - [4] E. Braaten and S. Fleming Phys. Rev. Lett **74** 3327 (1995).
 - [5] P. L. Cho and M. B. Wise, Phys. Lett. B **346** 129 (1995); A. K. Leibovich, Phys. Rev. D **56** 4412 (1997); M. Beneke and M. Kramer, Phys. Rev. D **55** 5269 (1997); E. Braaten, B. A. Kniehl and J. Lee, Phys. Rev. D **62** 094005 (2000).
 - [6] T. Affolder et al. [CDF Collaboration], Phys. Rev. Lett. **85** 2886 (2000).
 - [7] R. A. Briere, et al, CLEO Collaboration, Phys. Rev. D **70** 072001 (2004).
 - [8] Shi-yuan Li, Qu-bing Xie and Qun Wang, Phys. Lett. B **482** 65 (2000).
 - [9] Kingman Cheung, Wai-Yee Keung and Tzu Chiang Yuan, Phys. Rev. D **54** 929 (1996).
 - [10] C. W. Bauer, S. Fleming and M. Luke, Phys. Rev. D **63** 014006 (2001).
 - [11] C. W. Bauer, S. Fleming, D. Pirjol and I. W. Stewart, Phys. Rev. D **63** 114020 (2001).
 - [12] C. W. Bauer and I. W. Stewart, Phys. Lett. B **516** 134 (2001).
 - [13] C. W. Bauer, D. Pirjol and I. W. Stewart, Phys. Rev. D **65** 054022 (2002).
 - [14] S. Fleming, A. K. Leibovich, and T. Mehen, Phys. Rev. D **68** 094011 (2003).
 - [15] C. Bobeth, B. Grinstein, and M. Savorov, Phys. Rev. D **77** 074007 (2008).
 - [16] S. Fleming, A. K. Leibovich, Phys. Rev. D **67** 074035 (2003).
 - [17] E. Braaten and Y. Q. Chen, Phys. Rev. D **54** 3216 (1996).
 - [18] I. Z. Rothstein and M. B. Wise, Phys. Lett. B **402**, 346 (1997).
 - [19] S. Fleming, A. H. Hoang, S. Mantry and I. W. Stewart, Phys. Rev. D **77** 114003 (2008).
 - [20] A. K. Leibovich, Z. Ligeti and M. B. Wise, Phys. Lett. B **539** 242 (2002).
 - [21] P. Cho and A. K. Leibovich, Phys. Rev. D **53** 150 (1996).
 - [22] S. Fleming, O. F. Hernandez, I. Maksymyk and H. Nadeau, Phys. Rev. D **55** 4098 (1997).